NeuroImage 238 (2021) 118263

Contents lists available at ScienceDirect

NeuroImage

journal homepage: www.elsevier.com/locate/neuroimage

Dynamic inter-brain synchrony in real-life inter-personal cooperation: A functional near-infrared spectroscopy hyperscanning study

Rihui Li[a,1,*], Naama Mayseless[a,1], Stephanie Balters[a], Allan L. Reiss[a,b]

[a] Center for Interdisciplinary Brain Sciences Research, Department of Psychiatry and Behavioral Sciences, Stanford University School of Medicine, Stanford, CA 94305, USA

[b] Departments of Radiology and Pediatrics, Stanford University School of Medicine, Stanford, CA 94305, USA

ARTICLE INFO

Keywords:
Hyperscanning
fNIRS
Cooperation
Dynamic functional connectivity
Brain state

ABSTRACT

How two brains communicate with each other during social interaction is highly dynamic and complex. Multi-person (i.e., hyperscanning) studies to date have focused on analyzing the entire time series of brain signals to reveal an overall pattern of inter-brain synchrony (IBS). However, this approach does not account for the dynamic nature of social interaction. In the present study, we propose a data-driven approach based on sliding windows and k-mean clustering to capture the dynamic modulation of IBS patterns during interactive cooperation tasks. We used a portable functional near-infrared spectroscopy (fNIRS) system to measure brain hemodynamic response between interacting partners (20 dyads) engaged in a creative design task and a 3D model building task. Results indicated that inter-personal communication during naturalistic cooperation generally presented with a series of dynamic IBS states along the tasks. Compared to the model building task, the creative design task appeared to involve more complex and active IBS between multiple regions in specific dynamic IBS states. In summary, the proposed approach stands as a promising tool to distill complex inter-brain dynamics associated with social interaction into a set of representative brain states with more fine-grained temporal resolution. This approach holds promise for advancing our current understanding of the dynamic nature of neurocognitive processes underlying social interaction.

1. Introduction

Cooperation is a critical element of human social interaction and a key factor driving factor for economic growth and social progress. In particular, cooperation between two or more individuals can facilitate complex problem-solving and creativity (Xue et al., 2018). This type of social interaction has been recognized as one of the pivotal characteristics that fundamentally distinguish us from other species and is represented by the development of the relatively larger neocortex in the human brain (Dunbar, 2009). Understanding how one's brain communicates with another during social interaction is not only important for understanding our social nature but also provides critical reference to clarify the neurobiological basis of social-deficit-linked brain disorders such as autism spectrum disorder.

Recent development of brain imaging technologies, especially functional magnetic resonance imaging (fMRI), has enabled researchers to noninvasively study brain activity and significantly deepened our understanding of the neural basis of cognitive processes contributing to social interactions (Hagan et al., 2008; Nguyen et al., 2019; Fang et al., 2020; Matusz et al., 2019; Nastase et al., 2020). Hyperscanning, a method that features simultaneous measurement of brain activity from multiple individuals, has been recently proposed to study social interactions using advanced brain imaging techniques, including fMRI (Bilek et al., 2015; Lee et al., 2010) and electroencephalography (EEG) (Babiloni and Astolfi, 2014; Lindenberger et al., 2009). Hyperscanning experiments involving multiple individuals allow researchers to directly assess the social interaction of two (or more) brains compared to the traditional single person study design (Dikker et al., 2017; Yang et al., 2020). In particular, by using hyperscanning, we can measure the strength of brain-to-brain synchronizations, termed as inter-brain synchrony (IBS), to identify regional connections and inter-brain networks that are closely related to social interactions. For example, the prefrontal cortex (PFC), dorsolateral prefrontal cortex (DLPFC) and temporoparietal junction (TPJ) have been implicated as brain regions important for tasks involving cooperation and social interactions (Chaminade et al., 2012; Decety et al., 2004; Decety and Lamm, 2007). Despite the compelling developments in neuroimaging allowing for multi-person studies, these techniques face some inherent limitations restricting a more naturalistic and real-life social interaction design. For example, fMRI is costly to perform, highly sensitivity to body-motion artifacts, and requires a rigorous measurement experimental setting, while EEG is also highly vulnerable

* Corresponding author.
E-mail address: rihuili@stanford.edu (R. Li).

[1] These authors contributed equally to this work.

https://doi.org/10.1016/j.neuroimage.2021.118263.
Received 13 February 2021; Received in revised form 24 May 2021; Accepted 10 June 2021
Available online 11 June 2021.

to motion artifacts and has very poor spatial resolution due to volume conductivity problems (Zhang et al., 2006; Li et al., 2019, 2020a).

To bridge this gap, functional near-infrared spectroscopy (fNIRS) has been used as an alternative or complement to fMRI and EEG to study IBS. As a noninvasive optical imaging technique, fNIRS measures changes in cortical oxy- hemoglobin (HbO) and deoxy-hemoglobin (HbR) concentrations that are coupled with neuronal metabolic activity (Cui et al., 2011; Li et al., 2020c). Technically, fNIRS offers several advantages over fMRI and EEG, including reasonable spatial resolution and greater resilience to motion artifacts, which permits investigation of real-time brain dynamics in more naturalistic settings (Li et al., 2017; Jiang et al., 2012). To date, a number of studies have applied fNIRS-based hyperscanning to explore IBS under various social interactions, especially during inter-personal cooperation (Hirsch et al., 2017, 2018; Scholkmann et al., 2013). These hyperscanning studies have reported significant IBS alterations in the PFC, DLPFC, superior frontal cortex (SFC), superior temporal gyrus (STG), and TPJ between individuals while they were engaging in cooperation tasks (Cheng et al., 2015; Cui et al., 2012; Mayseless et al., 2019; Jiang et al., 2012; Funane et al., 2011; Pan et al., 2018). Among the majority of fNIRS-based hyperscanning studies, wavelet transform coherence (WTC) has been typically adopted to assess IBS during social interactions, wherein the coupling of two brain regions is assessed in both the time and frequency domain (Cui et al., 2012). Using different tasks, recent studies have showed that IBS during social interaction was not only spatially related to key brain regions but also dynamically varying across the task conditions. For instance, several studies showed that key IBS patterns during face-to-face teaching and learning was observed specifically at the left TPJ as well as PFC (Jiang et al., 2015; Pan et al., 2020). By averaging the WTC values of the same task block/condition from selected ROIs, Jiang et al. (2015) reported that the IBS for the leader–follower pairs was significantly higher in the left TPJ during verbal communication compared to non-verbal communication. Similarly, Pan et al. (2020) found that IBS strength between instructor and learner at the PFC was positively correlated with learning outcomes using a scaffolding strategy compared to a non-scaffolding strategy. Regarding inter-personal cooperation tasks, our recent hyperscanning study reported that IBS between different regions, such as PFC-TPJ and PFC-STG, were significantly related to cooperation performance and demonstrate a time-varying quality during the scan (Mayseless et al., 2019). For an overview of fNIRS hyperscanning studies, we refer the reader to the following references (Balters et al., 2020; Czeszumski et al., 2020).

Despite current progress obtained by fNIRS hyperscanning techniques, we argue that the assessment of IBS has been limited, in large part, by an implicit assumption of spatial and temporal stationarity throughout the measurement period (Zhang et al., 2020). Previous assessment of brain connectivity from fMRI and EEG, particularly during resting-state/task-free periods, has revealed numerous lines of evidence about the macro-scale spatiotemporal organization of the brain. It has been shown that spontaneous activity or task-evoked fluctuations are highly dynamic and can vary over periods of tens of seconds (Allen et al., 2014; Fang et al., 2020). These variations can be characterized as a series of recurring modular sub-networks of the brain response over time. Regarding social interaction, a recent review of hyperscanning summarized two main IBS modular networks typically involved in interpersonal interaction, the mirror neuron system (MNS) including the inferior frontal gyrus (IFG), inferior parietal lobule (IPL), and the SFG, and the mentalizing system (MS) consisting of the TPJ, precuneus and PFC. These two sub-networks complement one another in processing social information to allow cooperation, empathy and synchronization or to contravene such processes (Wang et al., 2018). Taken together, it is suggested that the focus of brain functional connectivity analysis may be shifted away from localizing single brain regions and toward characterization of dynamic coactivation patterns among two or more regions, that is, modular sub-networks. Conversely, most existing fNIRS-based hyperscanning studies have focused on assessing participant dyad's IBS at a single brain region/channel pair using temporal data obtained across the entire study. As well, the magnitude of IBS is typically obtained by averaging coherence within a manually segmented block/condition, an approach that might be too subjective to derive the intrinsic time-recurring brain sub-networks involved in social interactions. Thereby, we argue that traditional fNIRS hyperscanning analysis might decrease the spatiotemporal scale of the data, and likely hinder our ability to extract more fine-grained network-level information pertaining to brain dynamics and transitions. Accordingly, our current understanding of the IBS during social interaction is likely incomplete. Advancing our knowledge in this area requires novel tools that effectively capture more intrinsic brain dynamics in a high spatiotemporal manner for uncovering IBS patterns that cannot be discovered through traditional fNIRS hyperscanning analysis.

In the study presented here, we utilized previously published data (Mayseless et al., 2019) and proposed a novel data-driven approach to track the dynamic IBS patterns associated with real-life social interaction. Twenty healthy dyads participated in two interactive cooperation tasks (creative design task and model building task), while their brain activity was recorded using a portable fNIRS system. Dynamic IBS networks of each dyad during each of the cooperation tasks were constructed using a sliding window strategy and K-means clustering algorithm. We hypothesized that IBS between the dyad will evolve in a structured, time-sensitive manner as individuals undergo interactive cooperation during the tasks, indicating transient and functionally distinct brain states.

2. Materials and methods

2.1. Participants

The data used in this study was a subset of the data published in our previous hyperscanning study (Mayseless et al., 2019). There were 28 dyads participating in our original study, in which 3 dyads were excluded due to very noisy data across most channels and 5 dyads were further excluded due to exclusion of region of interest (ROI, see Section 2.5). Thereby, participants in this study were 40 healthy adults (20 males, age: 32.09 ± 6.95) resulting in 20 dyad pairs (5 male-male pairs, 7 male-female pairs, and 8 female-female pairs). All dyads were unacquainted with each other before joining the experiment. All participants were right-handed, healthy, and with normal or corrected to-normal vision. The research was approved by the Stanford University Institutional Review Board and performed in accordance with the Declaration of Helsinki. Participants were fully informed about the purpose of the research and provided written, informed consent prior to participation.

2.2. Cooperation tasks

Participants in each dyad were seated in front of each other on opposite sides of a square table. All dyads participated in two different cooperation tasks, including one 10-min creative design task and one 10-min 3D model building task. The order of the creative design and model building sessions were counterbalanced across participant dyads. During the creative design task, dyads were asked to work together to design a product that would motivate people to vote (Fig. 1A). The product could be of any design or format. After the completion of the creative design task, dyads would need to explain their product to an investigator. During the 3D model building task, dyads were asked to work together to build a commercially available 3D puzzle of an airplane by following the instruction of the puzzle within 10 min (Fig. 1B).

2.3. Team-level cooperation performance

Two trained raters independently watched the video recording of the cooperation tasks and scored the degree of cooperation in each dyad on

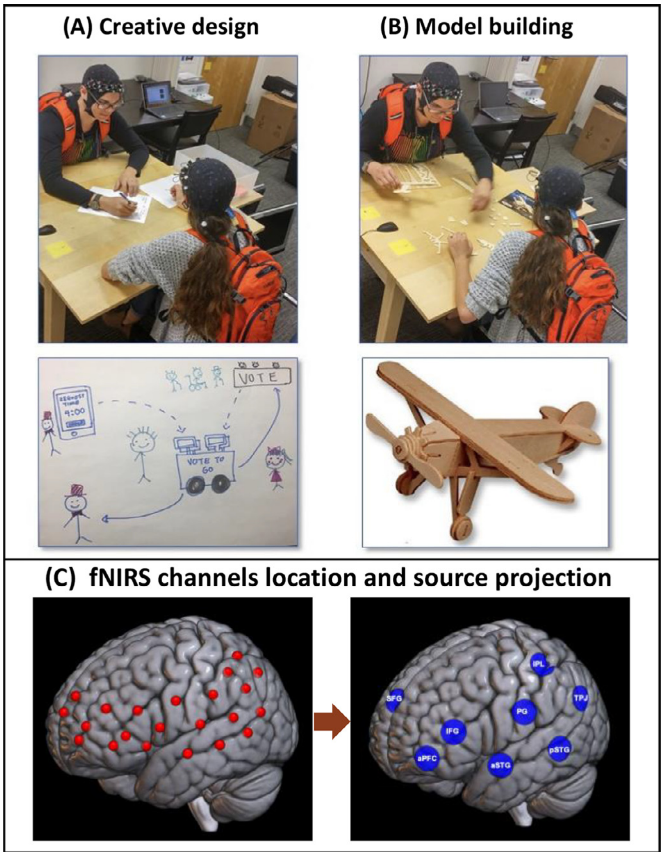

Fig. 1. Illustration of the study design. (A). The creative design task; (B). The 3D model building task; (C). Location of the fNIRS channels and region of interest (ROI) derived by source localization.

a 7-point Likert scale from 1 (poor cooperation) to 7 (very good cooperation). Cooperation was determined based on how well partners interacted, how much they interrupted each-other and how well conversation seemed to flow and ideas seemed related. Partners where either one person talked and the other did not listen, or both talked over each other in an unrelated matter received a lower score, while partners that were able to conduct a conversation and exchange ideas received higher scores. The mean of the scores given by two raters was used as the final cooperation performance of each dyad. Note that inter-rater reliability index (as measured by Intra Class Correlation Coefficient (ICC)) was satisfactory for all measures (creative design task ICC: 0.88, model building task ICC: 0.77).

2.4. Functional NIRS data acquisition

Cortical hemodynamic activity of each participant was recorded using a continuous wave fNIRS system (NIRSport Tandem, NIRX, Germany) with a sampling frequency of 7.81 Hz. Thirty-two optodes (16 sources $\times$ 16 detectors) were divided between the two participants of each dyad resulting in 16 optodes per participant. A total of 22 fNIRS channels were placed over the left PFC, temporal and parietal regions of each participant according to the international 10–20 EEG placement system (Fig. 1C). Plastic connectors were placed between each source/detector pair that constituted a recording channel to maintain an estimated 3 cm channel length.

2.5. Functional NIRS data analysis

Data were analyzed using the HOMER2 package in MATLAB and customized MATLAB-based script (Huppert et al., 2009). Briefly, the raw fNIRS data were first converted to optical density. After that, motion artifacts were removed from the optical density using a wavelet-based method (Molavi and Dumont, 2012). The concentration changes of HbO and HbR were then computed according to the Modified Beer-Lambert Law. The obtained HbO and HbR signals were further inspected for remaining noise using a correlation-based method (Cui et al., 2010), from which noisy channels were excluded from further analysis. Note that post-analysis in this study was solely based on HbO, since HbO signal is known to be more robust and sensitive than HbR to task-associated changes (Plichta et al., 2006; Ferrari and Quaresima, 2012). To estimate the regions of interest (ROI) that were covered by the fNIRS channels, we projected all fNIRS channels onto the cortical surface based on their MNI coordinates from the scalp surface using an automatic anatomical labeling method (Tzourio-Mazoyer et al., 2002). All channels that shared a common fNIRS source were averaged together resulting in 8 ROIs centered on source locations, including: (1) Superior Frontal Gyrus (SFG), (2) Anterior prefrontal cortex (aPFC), (3) Inferior frontal gyrus (IFG), (4) Anterior Superior Temporal Gyrus (aSTG), (5) precentral gyrus (PG), (6) Posterior Superior Temporal gyrus (pSTG), (7) Inferior Parietal Lobule (IPL) and (8) Temporoparietal junction (TPJ). Channels within the same ROI were averaged before further analysis. Note that we focused on these regions since they are the key components of the MNS and MS systems and have been shown to be involved in verbal communication, cooperation through body language (Jiang et al., 2012), cooperation in joint singing (Osaka et al., 2015) and creativity using structural, functional and brain dynamics analysis (Gonen-Yaacovi et al., 2013; Boccia et al., 2015; Beaty et al., 2019).

2.6. Dynamic inter-brain synchrony (IBS) states analysis

As illustrated in Fig. 2, the dynamic IBS analysis consisted of three key components: 1) IBS computation, 2) temporal segmentation using a sliding window, and 3) characterization of dynamic IBS (dIBS) states using k-means clustering algorithm.

2.6.1. Inter-brain synchrony (IBS) analyses

Wavelet Transform Coherence (WTC) was used to assess the IBS between the two fNIRS time series obtained from each participant in a dyad. A more detailed introduction of WTC can be found in (Grinsted et al., 2004). Briefly, WTC can identify locally phase locked behavior between two time-series by measuring cross-correlation between the time-series as a function of frequency and time. It has been shown in previous fNIRS hyperscanning studies that WTC can reveal meaningful IBS patterns during cooperation tasks (Cui et al., 2012; Baker et al., 2016). In each dyad, WTC was calculated between each ROI of one participant and all ROIs of the other participant on the HbO time series. The IBS between same ROI pairings were then averaged. For example, the IBS between PFC (participant 1) and TPJ (participant 2) was averaged with the IBS between PFC (participant 2) and TPJ (participant 1). This resulted in a total of 36 inter-brain connections for each dyad. While some studies have taken the approach of investigating IBS between the same regions (region A-region A only) (Cui et al., 2012; Jiang et al., 2015), others have taken the approach of investigating all possible IBS combinations. This research shows that task-evoked IBS patterns are observed not only between the same region but also across different regions of the participants during social interaction (Lu et al., 2019; Mayseless et al., 2019). Here we adopted the second approach and therefore have included all IBS regional pairings as described above. To be consistent with our previous study using the same paradigm (Mayseless et al., 2019), we selected the WTC values within a task-related frequency band of 0.015–0.15 Hz. This frequency band also excluded high- and low-frequency noise, such as cardiac pulsation ($\sim$1 Hz) and respiration (about 0.2–0.3 Hz), all of which are likely to be non-contributory to the measured hemodynamic response. The IBS of each ROI pair was then defined as the mean coherence value across

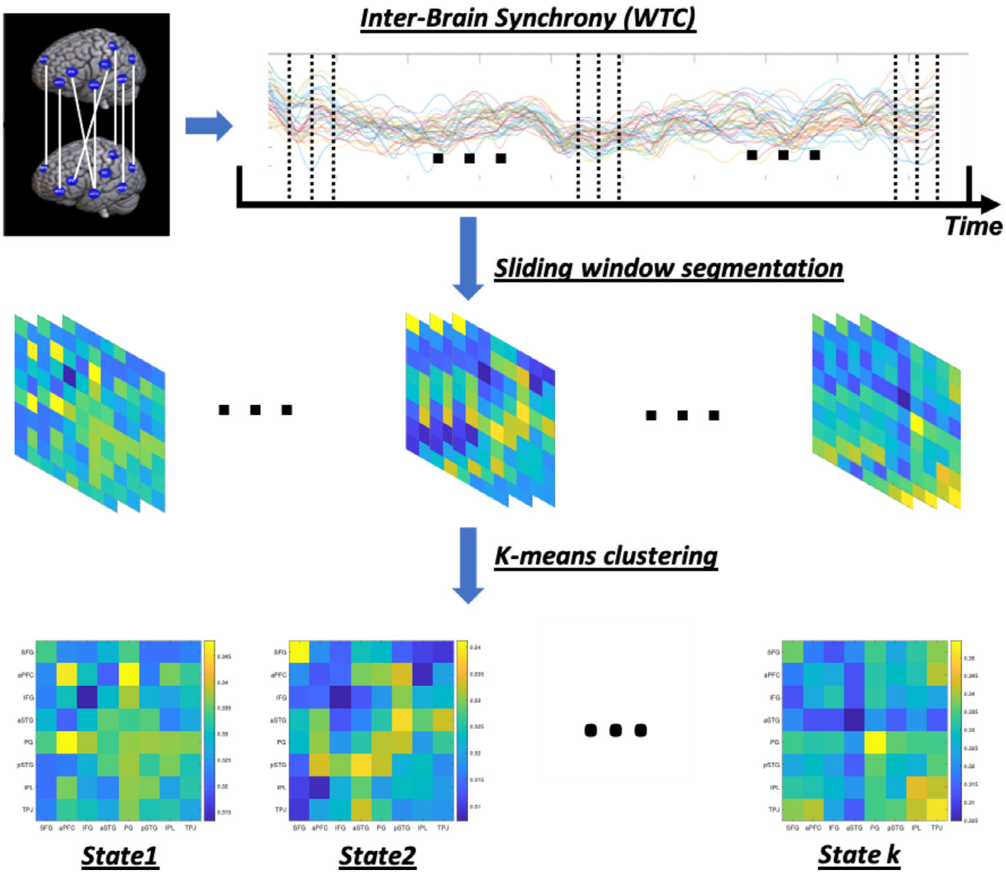

Fig. 2. Pipeline of the dynamic inter-brain synchrony states analysis.

the task in the selected frequency band and converted to z scores using Fisher z-transformation.

2.6.2. Dynamic IBS network segmentation

The creative design task and model building task were analyzed separately. As shown in Fig. 2, the IBS calculated by WTC across the entire task duration for each dyad was segmented using a sliding window-based approach (Allen et al., 2014), representing a series of windowed IBS matrices along the task period. The window size was set to 15 s and shifted in an increment of 1 s along the entire task. Within each time window, WTC values between the same pair of ROIs were averaged, resulting in an IBS matrix for each time window. The 10-min measurement duration was then segmented into a series of windowed IBS matrices (8 ROIs × 8 ROIs × 571 windows) for each dyad.

2.6.3. Characterization of dynamic IBS states

To characterize the dynamic IBS (dIBS) states during cooperation tasks, we applied a k-means clustering approach to the concatenated windowed IBS matrices averaged across the group. The k-means clustering approach can estimate the similarity between the windowed IBS matrices and identifies various clusters representing distinct IBS states derived from these windowed IBS matrices. Similar to previous studies, the number of clusters was determined using the elbow criterion of the cluster cost, computed as the ratio between within-cluster distance to between-cluster distance (Allen et al., 2014; Fang et al., 2020). We can compute the cost for different k values (e.g., from 1 to 15), and then plot these cost values as a function of the cluster number (see Fig. S1 in Supplementary data). With this approach, we sought to minimize the within-cluster distance and maximize the between-cluster distance, while controlling the number of the clusters. The appropriate number of k is generally selected at the elbow of the curve, optimally balancing the cluster cost and cluster number. In each iteration of cluster estimation, we estimated the similarity between the windowed IBS matrices using the L1 distance function (Manhattan distance) and repeated 1000 times to decrease chances of escaping local minima, with randomly initialized centroid positions. Cluster centroids obtained from the group-averaged IBS matrices were then used as the initial centroids for the individual dyad-level clustering analysis, resulting in final dIBS states for each dyad and each cooperation task.

To identify the true task-related regional connections in each clustered dIBS state, we constructed a series of permuted IBS matrices as a 'baseline' for each dIBS state, i.e. an unrelated-paired-participants' IBS matrix as compared to the real-paired-participants' dIBS matrices. This was calculated by using the time series of two unrelated players from the whole participant group, i.e. two players from different dyads and cooperation tasks. Out of a large number of possible pairings, permuted IBS matrices were formed by randomly selecting a set of 400 unrelated pairs (permuted pairs). We then performed a series of two-sample t tests on single regional connection level between individual dIBS matrices and the permuted IBS matrices to identify significant task-related regional connection in the dIBS matrices.

2.7. Statistical analysis

The properties of dIBS states were characterized by three metrics: fractional windows of each state, number of transitions between states, and global efficiency of each state. Fractional windows are defined as the percentage of total windows a dyad spent in each dIBS state (Allen et al., 2014). The number of transitions represents the total number of switches between any two states during the task. The global efficiency is an elementary graph-based metric that represents the integration of the entire network, reflecting how active and efficient a network can share information between regions (Li et al., 2020b). Repeated analysis of variance (ANOVA) was used to assess whether there were significant

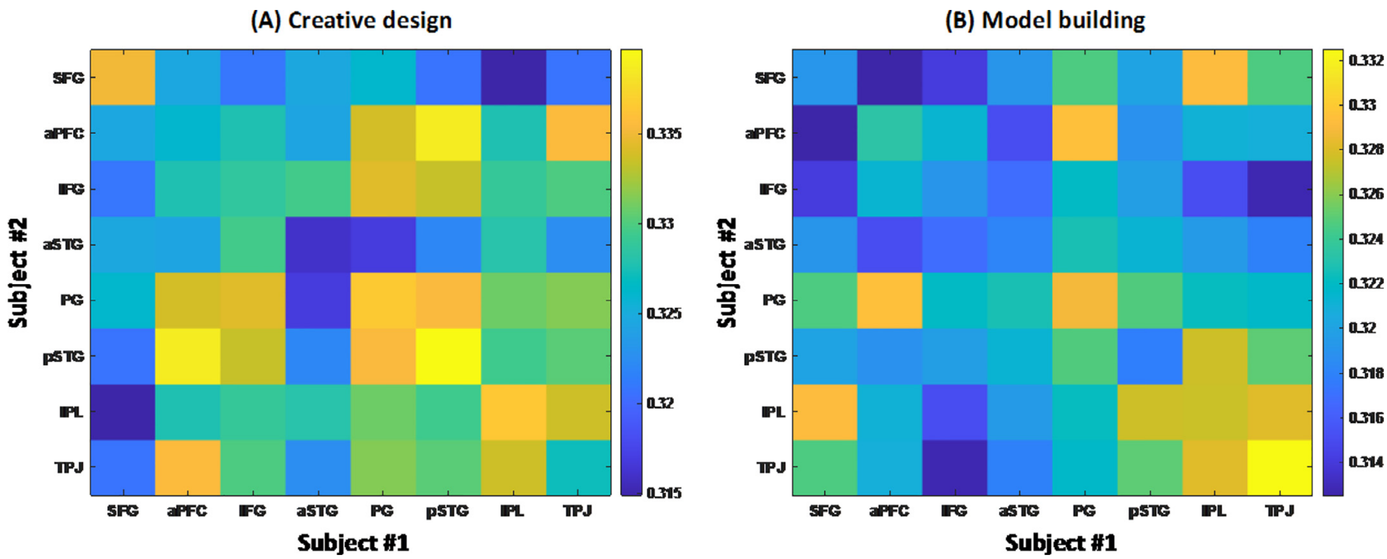

Fig. 3. The group-averaged static IBS networks (averaged across entire task duration) of the creative design task (A) and the 3D model building task (B).

Table 1
Statistical characteristics of the properties of dIBS states during creative design and 3D model building task.

Creative design task								
IBS measures	State 1	State 2	State 3	State 4	State 5	F value	p value	Effect size
Fractional windows (%)	19.9 ± 7.5	17.1 ± 7.4	21.2 ± 4.8	21.2 ± 6.4	20.6 ± 6.0	1.636	0.172	0.07
Global efficiency	0.24 ± 0.02	0.00 ± 0.00	0.18 ± 0.02	0.13 ± 0.01	0.01 ± 0.00	413.3	< 0.0001	0.95
State transitions			6.6 ± 1.8			/	/	
Model building task								
IBS measures	State 1	State 2	State 3	State 4	State 5	F value	p value	Effect size
Fractional windows (%)	20.2 ± 5.8	21.8 ± 5.7	20.0 ± 5.2	17.8 ± 4.7	20.2 ± 6.4	0.707	0.590	0.03
Global efficiency	0.01 ± 0.00	0.09 ± 0.01	0.07 ± 0.01	0.06 ± 0.01	0.01 ± 0.00	233.6	<0.0001	0.91
State transitions			6.5 ± 1.4			/	/	

differences between these dIBS states in terms of their properties during each cooperation task. In addition, a graph-based metric, termed as strength, was applied to assess the excitability of each brain region within each dIBS state. Specifically, the strength of a region is defined as the numerical sum of IBS connected to this region, which indicates its importance in the network (Li et al., 2020b). Finally, Pearson's correlations were computed between the properties of dIBS states and cooperation performance for each cooperation task (corrected by false discovery rate).

3. Results

3.1. Dynamic inter-brain synchrony states in creative design cooperation task

Through the k-means clustering analysis, five distinct dIBS states that were recurrent throughout individual dyad-level and across dyads were obtained for the creative design task and the model building task, separately. Compared to the static IBS network which is the average IBS across the entire task period without segmenting or clustering (Fig. 3A), the five dIBS states revealed modular organization including different IBS components (Fig. 4 and Table 1). As seen in Table 1, fractional windows of all dIBS states across the task ran from 17.1%–21.2% with no significant difference between them ($F = 1.636$, $p = 0.172$, effect size = 0.07). We also examined the temporal dynamics of these dIBS states using the occurrence rate as a function of time, defined as the percentage of each state is represented at current time window. When looking at occurrence rates over time (Fig. 4, right panel), the creative design task tended to be dominated by a sequentially single state for a certain period before switching to the next state.

In order to test which regional connections within each dIBS state were selective to the cooperation tasks we conducted a permutation test comparing real dyads to permuted dyads as described in the methods section. As shown in Fig. 5, during the creative design task, state 1, which accounted for 19.9% of all time windows, showed broader and denser IBS within and between the frontal, temporal and the parietal cortices. State 3 (21.2%) and state 4 (21.2%) presented the same occurrence rate, but showed distinct modular organization diverging substantially from each other. The dIBS pattern in state 3 tended to focus more on frontal and parietal cortices, while state 4 involved more IBS in the frontal and temporal cortices. Conversely, state 2 (17.1%) and state 5 (20.6%) only included very limited IBS and regions, however, both states accounted for equivalent occurrence rate as other states across the creative design task, as indicated by the repeated ANOVA test (Table 1). Statistical analysis also indicated that there was significant difference in global efficiency among the dIBS states, as evidenced by the repeated ANOVA test ($F = 413.3$, $p < 0.0001$, effect size = 0.97) and post hoc paired t-test between any two dIBS states (all p values < 0.0001).

3.2. Dynamic inter-brain synchrony states in model building cooperation task

The group-level dIBS states and their temporal occurrence patterns during the model building task are shown in Fig. 6. Each dIBS state remained significantly distinct relative to the static IBS network (Fig. 3B) and followed a sequential occurrence pattern along the task duration

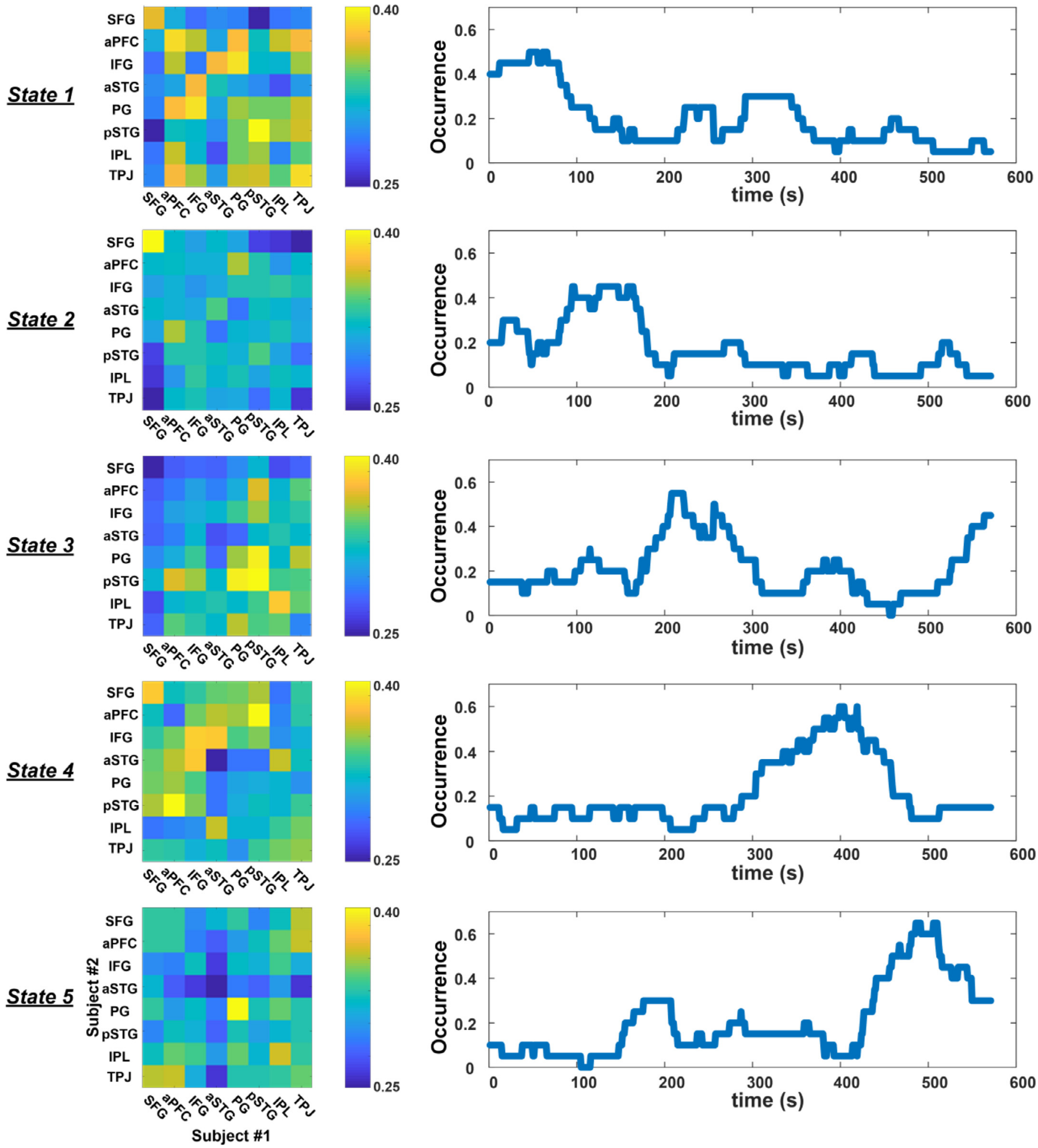

Fig. 4. Dynamic inter-brain synchrony (dIBS) states (left panel) and corresponding occurrence rate (right panel) during the creative design task.

(Fig. 6). Fractional windows of dIBS across the task ran from 17.8%–21.8% with no significant difference between them as indicated by a repeated ANOVA ($F = 0.707$, $p = 0.590$, effect size = 0.03). When looking at occurrence rates over time (Fig. 6, right panel), similar to the creative cooperation task, occurrence rates tended to be dominated by a sequentially single state for a certain period before switching to the next state.

The permutation test comparing real dyads to permuted dyads in model building task revealed that connections between regions tended to be less dense compared to those in creative design task (Figs. 5 and 7). Briefly, as can be seen in the strength of IBS connection presented in Figs. 5 and 7, state 1 and state 5 mainly presented with stronger excitability (assessed by strength) and more IBS in frontal cortex, while the majority of IBS in state 2 were between temporal and parietal cortices.

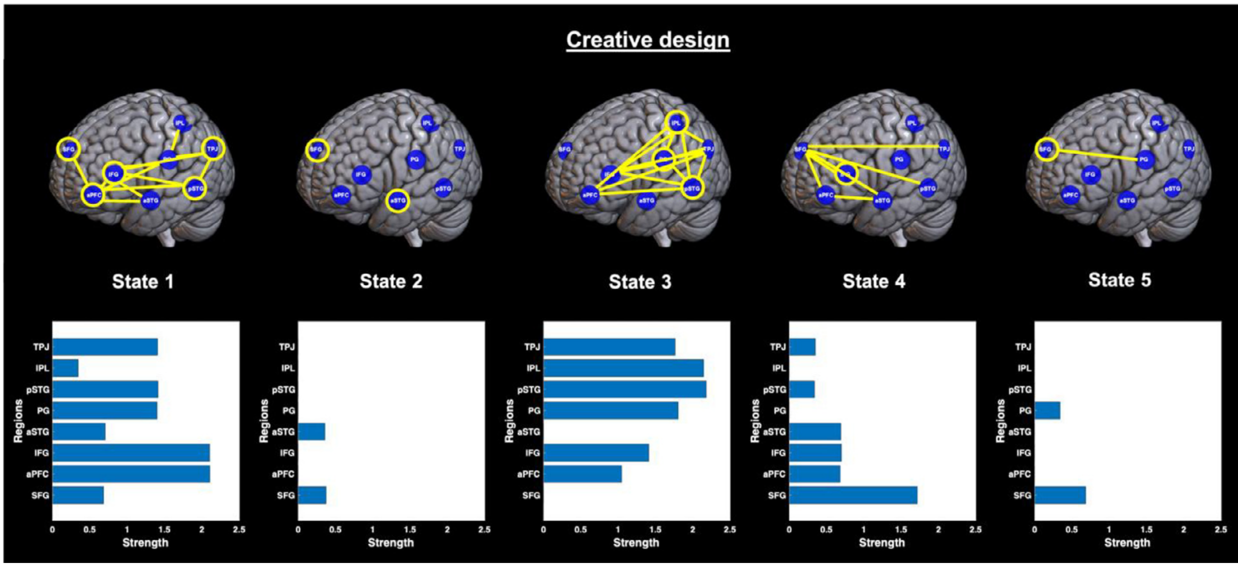

Fig. 5. Dynamic inter-brain synchrony (dIBS) states during creative design task (top, after permutation test) and the group-averaged strength of each region (bottom). Note that each IBS connection within each brain state represents the parallelly averaged IBS within the dyad for an intuitive demonstration of each dIBS state's structure.

In addition, state 3 displayed strong IBS within the parietal cortex and consistent communication with SFG. State 4 revealed a main modular organization in the temporal-parietal area, but also has a direct connection with the anterior part of the frontal cortex (aPFC).

Another measure of dynamic progression of dIBS states was the number of transitions between dIBS states during each cooperation task. The transitions between all dIBS states during the model building task were 6.5 ± 1.4, which was not significantly different to the transitions during the creative design task (6.6 ± 1.8) after a paired t-test ($p = 0.844$).

Similar to the creative design task, there was significant difference in global efficiency among all dIBS states except the state 1 – state 5 pair ($p = 0.681$), as evidenced by the repeated ANOVA test ($F = 233.6$, $p < 0.0001$, effect size = 0.93) and post hoc paired t-test between any two dIBS states (all p values < 0.0001). The statistical characteristics of the properties of dIBS states in two cooperation tasks have been summarized in Table 1.

3.3. Relationship between dIBS states and cooperation performance

For the creative cooperation design task, the global efficiency of state 5 was positively correlated with the cooperation performance rating ($r = 0.649$, $p = 0.002$, corrected by Benjamini-Hochberg method). Within state 5, the IBS between SFG and PG was significantly correlated with cooperation performance ($r = 0.649$, $p = 0.002$, corrected by Benjamini-Hochberg method). Within state 1, IBS between dyad's IFG region was positively correlated with participants' cooperation performance ($r_{\text{IFG-IFG}} = 0.611$, $p_{\text{IFG-IFG}} = 0.004$, corrected by Benjamini-Hochberg method). We did not observe significant correlations between the properties of dIBS state and cooperation performance during the 3D model building task.

4. Discussion

Human brain activity is supported by complex networks with time-varying communications and network organization. The study presented here explored dynamic patterns of inter-brain synchrony (IBS) during two cooperation tasks using a data-driven approach based on sliding window and k-means clustering algorithm. To the best of our knowledge, our analysis is the first attempt to characterize dIBS states during naturalistic inter-personal social interaction, which provides a new perspective to the growing literature on fNIRS-based hyperscanning analysis. The proposed approach might enable researchers to dynamically capture modular network organization and transient brain states, expanding our knowledge of neural mechanisms underlying naturalistic inter-personal social interaction.

Understanding how the brain adapts and organizes in a dynamic manner is critical for elucidating the neural basis of social interaction. Compared to fMRI, fNIRS offers various potential advantages; it is highly portable, low cost, and more resilient to motion artifacts which, together, permit assessment of real-time brain dynamics and IBS in naturalistic settings. By generating a series of modular networks reflecting the dynamic interaction between two brains at the level of individual time frames, our approach provides a novel window for understanding the multi-aspect functional processing of typical inter-brain communication during complex and naturalistic cooperation tasks. More importantly, recent dynamic functional connectivity studies targeting single brain activity have demonstrated the feasibility of using similar methods to characterize atypical pathophysiological processes in clinical populations, such as Alzheimer's disease and Parkinson's disease (Niu et al., 2019; Fiorenzato et al., 2019). With this in mind, we hypothesize that this level of dynamic representation of transitions and organizations in IBS makes our approach useful for studying inter-person social interaction and potentially developing phenotypic biomarkers for social deficit-related brain disorders.

4.1. Creative cooperation task dIBS

Inter-personal creative cooperation is a bottom-up process which usually involves various aspects of cognitive control including, but not limited to, creative thinking, goal-directed memory retrieval, communication, and cooperation (Wang et al., 2018). Using the same data set and a static IBS analysis, we previously found increased IBS between three regions linking the creative cooperation process to the mirror neuron (MNS, including the IFG, IPL, and the superior temporal region) and mentalizing systems (MS, including the TPJ, precuneus and PFC) (Mayseless et al., 2019). The MNS generally reflects exaptation, the evolutionary "repurposing" of a system of gestural communication, to support both verbal and non-verbal communication and interaction

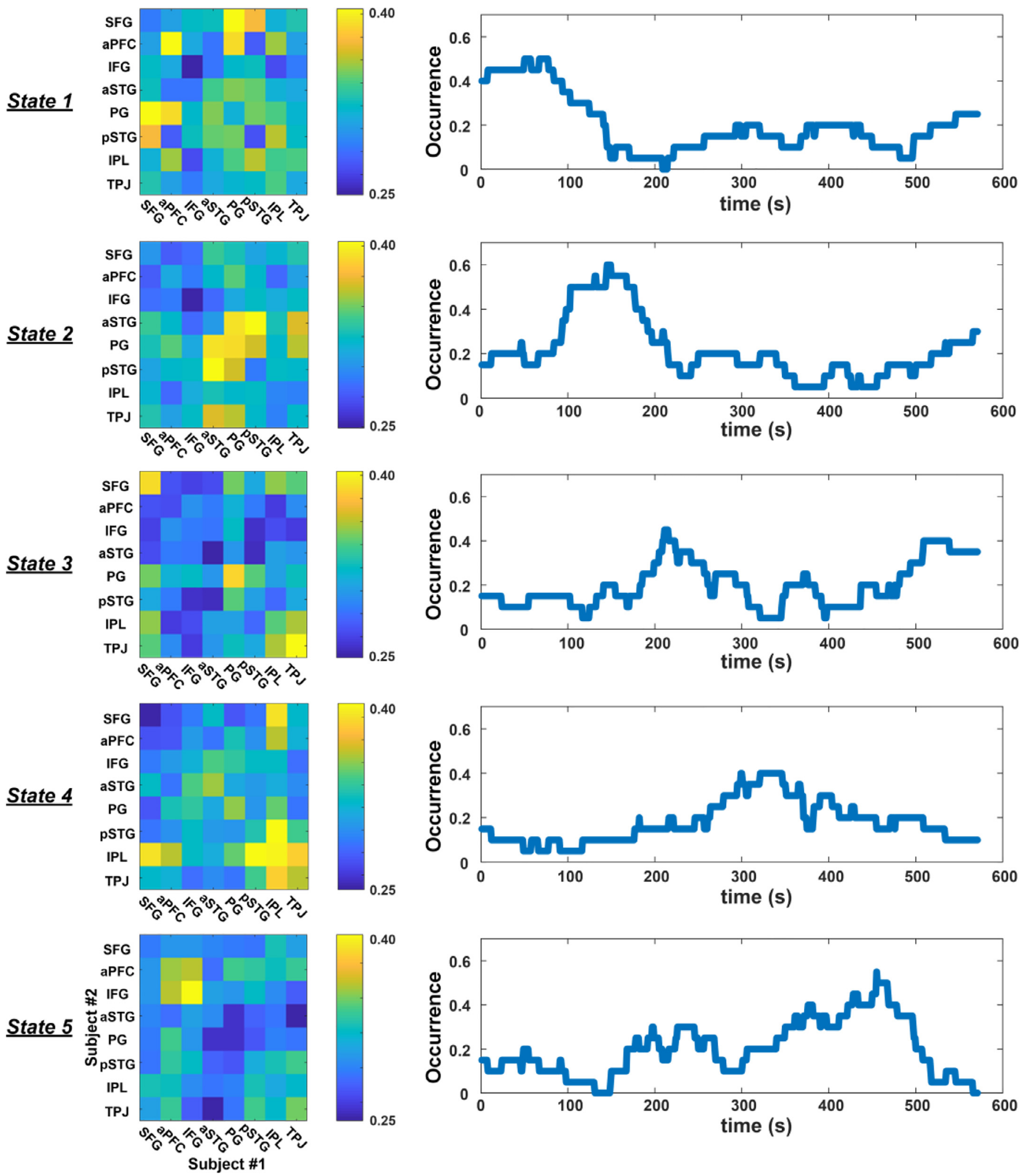

Fig. 6. Dynamic inter-brain synchrony (dIBS) states (left panel) and corresponding occurrence rate (right panel) during the 3D model building task.

(Dickerson et al., 2017). The MS is typically more active when one is trying to understand others' intentions and emotions based on gestures, behaviors and facial expressions (Frith and Frith, 2006). The new dynamic IBS analysis presented here extends prior knowledge of the network neuroscience of creative interaction by revealing the engagement of these brain networks in a finer time-varying manner. In particular, the dIBS state 1 presented with a broad IBS pattern similar to the static IBS study, depicting changes in IBS among the MNS and MS neural networks typically involved in social interaction. Following state 1, the dIBS state 2 shifted to more localized IBS between inter-brain SFG and between inter-

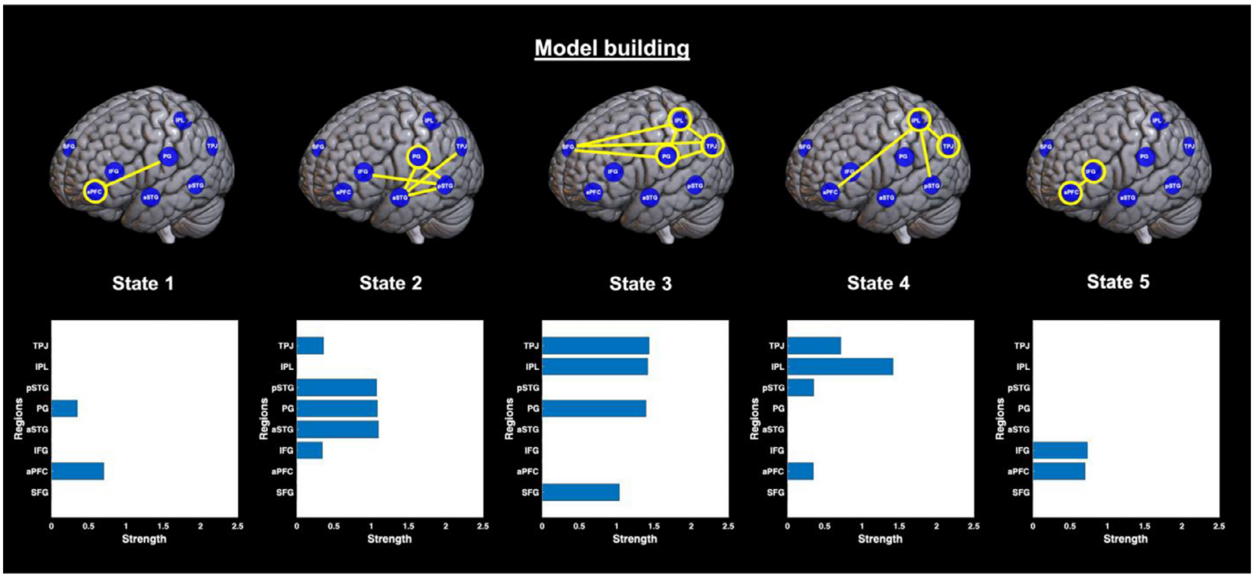

Fig. 7. Dynamic inter-brain synchrony (dIBS) states during the 3D model building task (top, after permutation test) and the group-averaged strength of each region (bottom). Note that each IBS connection within each brain state represents the parallelly averaged IBS within the dyad for an intuitive demonstration of each dIBS state's structure.

brain aSTG. The SFG is known to be involved in higher cognitive functions, particularly working memory and attention (du Boisgueheneuc et al., 2006), while the aSTG is an important component of language processing (Broca's area). This stage may indicate that the dyad tended to refine their ideas by interactive communication. State 3, occurring during the middle of the task, mainly involved active IBS in temporo-parietal lobe (PG, pSTG, IPL and TPJ) with few connections to the aPFC and IFG. State 4 displayed dominant IBS in prefrontal cortex and several connections between prefrontal cortex and aSTG/TPJ. This module here again demonstrated a coupling between MS and MNS, which was similar but relatively weaker compared to the components showed in state 1. In state 5, dIBS was only observed at inter-brain SFG and between the SFG and PG, a finding that suggests the need for cognitive control and executive function to finalize the product at the end of the task. Taken together, these sequential shifts among the dynamic IBS states may explain shifts in communication patterns and cooperation between individuals engaged in a creative, relatively unstructured, free-ranging task. Our findings thus extend the understanding of the dynamic properties of the MNS and MS during creative cooperation and potentially enable finer-grained analysis of human social interaction.

4.2. 3D model building cooperation task dIBS

How the IBS pattern varies in different inter-personal cooperation activities, regardless of static or dynamic characteristics, has not been well studied in previous research. To evaluate the applicability and specificity of the proposed dIBS method for understanding dynamic social interactions, we further analyzed the data collected from a different cooperation task involving the construction of a 3D model. The dIBS states identified during the model building task were clearly different from those observed during the creative design task (Fig. 6). The early state of the model building task did not involve complex interaction between MNS and MS as was the case in the creative task. Instead, state 1 only showed active IBS at the aPFC and between the aPFC and PG. The aPFC, located approximately in the dorsolateral prefrontal cortex (DLPFC), is typically related to executive functions such as goal maintenance and emotion regulation (Silvers et al., 2015; Curtis and D'Esposito, 2003), and the PG is responsible for motor function (Porro et al., 1996). The state 1 observed at the beginning of the task might be anticipated since participants were presented with a target for completing the model building task, which did not require complex processing of language, actions and emotion as they did at the beginning of the creative task. The central role of PG further extended through state 2 and state 3, where it displayed a IBS within the temporo-parietal lobe and the fronto-parietal lobe. Similar IBS between the aPFC and parietal lobe (IPL, TPJ) was also presented in state 4. Unlike the concurrent coupling of MNS and MS observed distinctly within state 1 during the creative design task, here, we observed a coupling between MNS and MS represented in states 2,3 and 4 in a sequential manner. State 5 was identified at the end of the task, and mainly included IBS between IFG and aPFC, which might indicate the participant's emotional response to the completion of the task since both the IFG and aPFC have been reported to be involved in emotion contagion and cognitive control over emotion (Ochsner et al., 2012).

4.3. Qualitative comparison between the creative design task and the model building task

While a directly quantitative comparison between the two cooperation tasks in terms of dIBS states is not available due to the different timing/duration of each state, we were still able to capture obvious differences between two tasks in a qualitative manner. Compared to the model building task, the creative design task appeared to recruit more complex and stronger IBS between multiple regions as evidenced by the strength of each region and their inter-region connections (Figs. 5 and 7), demonstrating a more active coupling of the MNS and MS systems. We can speculate that the distinct dIBS pattern observed in each task might be related to task demands. It is possible that the creative task provided to the dyads was an open-ended real-world problem, which required a more active creative thinking and social interaction between the dyad compared to the well-defined model building task. This assumption is supported by our recent study that stronger IBS between several regional connections were observed during creative task compared to the model building task (Mayseless et al., 2019). However, the interpretation of dIBS differences between two tasks should be undertaken with caution due to the distinct, yet complex multi-dimensional cognitive processing that occurs during these non-structured cooperation tasks. Instilling more fine-tuned temporal analysis of the neuroscience of social interaction is therefore needed in order to better understand the nuances of this complex human behavior. Here, we propose a novel method for IBS analysis that permits observation and measurement of the different stages of social interaction at the network level. In particular, the unique IBS states identified for each task can potentially help explicate behavioral aspects of the dyad's interaction during the task such as varying levels of cooperation, goal-oriented vs. open-ended type of task, communication demands and varying levels of social coordination. While the current study is limited in its behavioral analysis of the dyad's interaction, we propose that future studies use dynamic temporal analysis together with a more nuanced behavioral analysis of the interaction to derive meaningful insights.

4.4. Relationship between dIBS states and cooperation behavior

Very few neuroimaging studies have focused on the temporal dynamics of IBS or examined how the transition of different dIBS states may be associated with overall inter-personal cooperation. Our goal here was to introduce and test the added benefit of dynamical IBS analysis in explaining dynamical social interactions by evaluating the association between the network properties of dIBS and measures of social interaction performance such as cooperation. Specifically, we observed a significantly positive correlation between cooperation performance and the global efficiency of state 5 during the creative design task. The IBS between SFG and PG within state 5 was also significantly related to cooperation performance. Global efficiency is a measure of network integration that typically reflects how active and efficient a network can share information between regions. This might signify that stage 5, in particular the connection between SFG and PG, are more central for cooperation during creative cognition. Surprisingly, while increased IBS between aPFC and pSTG was found to be associated with better cooperation performance in our previous static IBS study (Mayseless et al., 2019), we did not observe this specific IBS in any dynamic state to be associated with cooperation performance. In fact, social interaction is a complex process that involves multiple aspects of neurocognitive function including emotion processing, working memory, communication, and executive function. We argue that, compared to conventional fNIRS hyperscanning analysis that generally targets the relation between single IBS strength and simple interaction performance (e.g., score of cooperation or competition), our approach targets the distinct aspects of the dynamic nature of social interaction by distilling complex brain dynamics associated with social interaction into a set of representative brain states with a more fine-grained temporal resolution. For example, in the creative task, the dIBS state 2 observed may reflect the demand of working memory and attention processing, while state 3 appeared more related to the participant's executive function, visuospatial processing and inference of emotions. That is, the identified dIBS states, from the view of brain sub-networks, provide direct evidence about complex multi-function processes during cooperation that cannot be observed by conventional hyperscanning analysis. Following this, it is not surprising to see that the dynamic property of most dIBS states was not significantly correlated with the dyad's overall cooperation performance in both tasks. Given the complex process of social interaction (e.g., emotion, working memory, commutation), a clear clarification of brain state-behavior associations is likely to require more complex coding strategies of the participants' dimensional cognitive and interaction states in future studies. We hope that future studies will be designed to more fully explicate the relationship between these dIBS states and their corresponding behaviors during social interaction.

4.5. Limitations

Several limitations should be recognized in the present study. First, dIBS analysis lacks a gold standard for selection of optimal window length. As an exploratory validation, we have separately used sliding window lengths of 10, 15, 30, and 60 s to examine the impact of varying window lengths on the dynamic IBS patterns. Results indicated that all dIBS patterns were generally consistent across different window lengths (see Figs. S2 and S3 in Supplementary data). We hope that more studies will be conducted in the future to validate the criteria for selection of window length in dynamic IBS analysis.

It is also worth noting that, while fNIRS can be seen as suited for social interaction studies due to its portability, low cost, increased resistance to movement artifact and higher temporal resolution than fMRI (Cui et al., 2011), it is also limited by its spatial resolution, penetration depth and signal-to-noise ratio (Yucel et al., 2021). Similar to most fNIRS hyperscanning studies, here we only adopted fNIRS channels with typical between-optode distance ($\sim$3 cm), an approach that may be contaminated to a certain degree by Mayer wave, blood pressure and other systematic artifacts (Yucel et al., 2021). Incorporating short channels in the data collection and analysis can mitigate this effect and improve the signal to noise ratio, thus providing more reliable analysis in the future. Despite the hardware limitation in our study, we also want to emphasize that the major contribution of the current study is to provide a novel data-driven approach to distill complex inter-brain dynamics associated with social interaction into a set of representative brain sub-networks with more fine-grained temporal resolution. The analysis framework proposed here can be directly adapted to hyperscanning studies with different types of data acquisition setup (e.g., with or without short channels), expanding our current analysis strategies for fNIRS hyperscanning data collected during various social interaction scenarios.

In terms of measurement coverage, while we only focused on brain regions known to be associated with IBS during cooperation tasks, the lack of a whole-head coverage may have hindered a more comprehensive understanding of dynamic IBS during social interaction. We plan to enlarge fNIRS brain coverage in future studies. Finally, the functional source localization of fNIRS channels here was performed using a generic head template based on the standard 10–20 electrode placement. Although the generic model still features a realistic anatomy, the variance of subject-specificity might blind the current method to individual differences in anatomy or cap setup. Considering this, it would be useful for future research to obtain subject-specific models through anatomical MRI or 3D digitization techniques, which can significantly improve the accuracy of source localization for each subject.

5. Conclusion

The data-driven approach presented in this study sheds light on the activity of dynamic IBS brain networks during naturalistic inter-personal cooperation scenarios. Our findings demonstrate that the nature of social cooperation can potentially be characterized using a more dynamic and modular approach. That is, the process of social interaction is not only modulated by time-varying IBS networks, but also via inter-brain communication between key regions within different dynamic IBS networks. This approach allows us to develop a better understanding of the dynamic process of naturalistic social interaction as seen through the lens of IBS.

Data and code availability statement

Data used in this study are not publicly available due to research data sharing restriction from the university but are available from the corresponding author on qualified request. Source code for this work is publicly available at (https://github.com/ericRHLi/dynamic-IBS-analysis.git).

Declaration of Competing Interest

The authors declare no conflict of interest.

Credit authorship contribution statement

Rihui Li: Conceptualization, Methodology, Formal analysis, Visualization, Data curation, Writing - original draft, Writing - review & editing. **Naama Mayseless:** Investigation, Formal analysis, Data curation, Writing - review & editing. **Stephanie Balters:** Methodology, Writing - review & editing. **Allan L. Reiss:** Writing - review & editing, Supervision, Funding acquisition.

Acknowledgments

This work was supported by a Hasso Plattner Design Thinking Research Program grant and gifts from the Albert Yu and Mary Bechmann Foundation and the Feldman Foundation.

Supplementary materials

Supplementary material associated with this article can be found, in the online version, at doi:10.1016/j.neuroimage.2021.118263.

References

Allen, E.A., Damaraju, E., Plis, S.M., et al., 2014. Tracking whole-brain connectivity dynamics in the resting state. Cereb. Cortex 24 (3), 663–676.
Babiloni, F., Astolfi, L., 2014. Social neuroscience and hyperscanning techniques: past, present and future. Neurosci. Biobehav. Rev. 44, 76–93.
Baker, J.M., Liu, N., Cui, X., et al., 2016. Sex differences in neural and behavioral signatures of cooperation revealed by fNIRS hyperscanning. Sci. Rep. 6, 26492.
Balters, S., Baker, J.M., Hawthorne, G., et al., 2020. Capturing human interaction in the virtual Age: a perspective on the future of fNIRS Hyperscanning. Front. Hum. Neurosci. 14, 588494.
Beaty, R.E., Seli, P., Schacter, D.L., 2019. Network neuroscience of creative cognition: mapping cognitive mechanisms and individual differences in the creative brain. Curr. Opin. Behav. Sci. 27, 22–30.
Bilek, E., Ruf, M., Schäfer, A., et al., 2015. Information flow between interacting human brains: identification, validation, and relationship to social expertise. Proc. Natl. Acad. Sci. 112 (16), 5207–5212.
Boccia, M., Piccardi, L., Palermo, L., et al., 2015. Where do bright ideas occur in our brain? Meta-analytic evidence from neuroimaging studies of domain-specific creativity. Front. Psychol. 6, 1195.
Chaminade, T., Marchant, J.L., Kilner, J., et al., 2012. An fMRI study of joint action-varying levels of cooperation correlates with activity in control networks. Front. Hum. Neurosci. 6, 179.
Cheng, X., Li, X., Hu, Y., 2015. Synchronous brain activity during cooperative exchange depends on gender of partner: a fNIRS-based hyperscanning study. Hum. Brain Mapp. 36 (6), 2039–2048.
Cui, X., Bray, S., Bryant, D.M., et al., 2011. A quantitative comparison of NIRS and fMRI across multiple cognitive tasks. Neuroimage 54 (4), 2808–2821.
Cui, X., Bray, S., Reiss, A.L., 2010. Functional near infrared spectroscopy (NIRS) signal improvement based on negative correlation between oxygenated and deoxygenated hemoglobin dynamics. Neuroimage 49 (4), 3039–3046.
Cui, X., Bryant, D.M., Reiss, A.L., 2012. NIRS-based hyperscanning reveals increased interpersonal coherence in superior frontal cortex during cooperation. Neuroimage 59 (3), 2430–2437.
Curtis, C.E., D'Esposito, M., 2003. Persistent activity in the prefrontal cortex during working memory. Trends Cogn. Sci. 7 (9), 415–423 Regul. Ed..
Czeszumski, A., Eustergerling, S., Lang, A., et al., 2020. Hyperscanning: a valid method to study neural inter-brain underpinnings of social interaction. Front. Hum. Neurosci. 14, 39.
Decety, J., Jackson, P.L., Sommerville, J.A., et al., 2004. The neural bases of cooperation and competition: an fMRI investigation. Neuroimage 23 (2), 744–751.
Decety, J., Lamm, C., 2007. The role of the right temporoparietal junction in social interaction: how low-level computational processes contribute to meta-cognition. Neuroscientist 13 (6), 580–593.
Dickerson, K., Gerhardstein, P., Moser, A., 2017. The Role of the Human Mirror Neuron System in Supporting Communication in a Digital World. Front. Psychol. 8, 698.
Dikker, S., Wan, L., Davidesco, I., et al., 2017. Brain-to-brain synchrony tracks real-world dynamic group interactions in the classroom. Curr. Biol. 27 (9), 1375–1380.
du Boisgueheneuc, F., Levy, R., Volle, E., et al., 2006. Functions of the left superior frontal gyrus in humans: a lesion study. Brain 129, 3315–3328 (Pt 12).
Dunbar, R.I., 2009. The social brain hypothesis and its implications for social evolution. Ann. Hum. Biol. 36 (5), 562–572.
Fang, F., Potter, T., Nguyen, T., et al., 2020. Dynamic reorganization of the cortical functional brain network in affective processing and cognitive reappraisal. Int. J. Neural. Syst. 30 (10), 2050051.
Ferrari, M., Quaresima, V., 2012. A brief review on the history of human functional near-infrared spectroscopy (fNIRS) development and fields of application. Neuroimage 63 (2), 921–935.
Fiorenzato, E., Strafella, A.P., Kim, J., et al., 2019. Dynamic functional connectivity changes associated with dementia in parkinson's disease. Brain 142 (9), 2860–2872.
Frith, C.D., Frith, U., 2006. The neural basis of mentalizing. Neuron 50 (4), 531–534.
Funane, T., Kiguchi, M., Atsumori, H., et al., 2011. Synchronous activity of two people's prefrontal cortices during a cooperative task measured by simultaneous near-infrared spectroscopy. J. Biomed. Opt. 16 (7), 077011.
Gonen-Yaacovi, G., de Souza, L.C., Levy, R., et al., 2013. Rostral and caudal prefrontal contribution to creativity: a meta-analysis of functional imaging data. Front. Hum. Neurosci. 7, 465.
Grinsted, A., Moore, J.C., Jevrejeva, S., 2004. Application of the cross wavelet transform and wavelet coherence to geophysical time series. Nonlin. Processes Geophys. 11, 561–566.
Hagan, C.C., Hoeft, F., Mackey, A., et al., 2008. Aberrant neural function during emotion attribution in female subjects with fragile X syndrome. J. Am. Acad. Child Adolesc. Psychiatry 47 (12) 1443-1354.
Hirsch, J., Adam Noah, J., Zhang, X., et al., 2018. A cross-brain neural mechanism for human-to-human verbal communication. Soc. Cogn. Affect. Neurosci. 13 (9), 907–920.
Hirsch, J., Zhang, X., Noah, J.A., et al., 2017. Frontal temporal and parietal systems synchronize within and across brains during live eye-to-eye contact. Neuroimage 157, 314–330.
Huppert, T.J., Diamond, S.G., Franceschini, M.A., et al., 2009. HomER: a review of time-series analysis methods for near-infrared spectroscopy of the brain. Appl. Opt. 48 (10), D280–D298.
Jiang, J., Chen, C., Dai, B., et al., 2015. Leader emergence through interpersonal neural synchronization. Proc. Natl. Acad. Sci. 112 (14), 4274–4279.
Jiang, J., Dai, B., Peng, D., et al., 2012. Neural synchronization during face-to-face communication. J. Neurosci. 32 (45), 16064–16069.
Lee, R.F., Dai, W., Dix, W., 2010. A decoupled circular-polarized volume head coil pair for studying two interacting human brains with MRI. Annu. Int. Conf. IEEE Eng. Med. Biol. Soc. 2010, 6645–6648.
Li, R., Li, S., Roh, J., et al., 2020a. Multimodal neuroimaging using concurrent EEG/fNIRS for poststroke recovery assessment: an exploratory study. Neurorehabil Neural Repair. 34 (12), 1099–1110.
Li, R., Nguyen, T., Potter, T., et al., 2019. Dynamic cortical connectivity alterations associated with Alzheimer's disease: an EEG and fNIRS integration study. Neuroimage Clin. 21, 101622.
Li, R., Potter, T., Huang, W., et al., 2017. Enhancing performance of a hybrid EEG-fNIRS system using channel selection and early temporal features. Front. Hum. Neurosci. 11, 462.
Li, R., Rui, G., Zhao, C., et al., 2020b. Functional network alterations in patients with amnestic mild cognitive impairment characterized using functional near-infrared spectroscopy. IEEE Trans. Neural. Syst. Rehabil. Eng. 28 (1), 123–132.
Li, R., Zhao, C., Wang, C., et al., 2020c. Enhancing fNIRS analysis using EEG rhythmic signatures: an EEG-informed fNIRS analysis study. IEEE Trans. Biomed. Eng..
Lindenberger, U., Li, S.C., Gruber, W., et al., 2009. Brains swinging in concert: cortical phase synchronization while playing guitar. BMC Neurosci. 10, 22.
Lu, K., Xue, H., Nozawa, T., et al., 2019. Cooperation makes a group be more creative. Cereb. Cortex 29 (8), 3457–3470.
Matusz, P.J., Dikker, S., Huth, A.G., et al., 2019. Are We Ready For Real-World Neuroscience?. MIT Press.
Mayseless, N., Hawthorne, G., Reiss, A.L., 2019. Real-life creative problem solving in teams: fNIRS based hyperscanning study. Neuroimage 203, 116161.
Molavi, B., Dumont, G.A., 2012. Wavelet-based motion artifact removal for functional near-infrared spectroscopy. Physiol. Meas. 33 (2), 259–270.
Nastase, S.A., Goldstein, A., Hasson, U., 2020. Keep it real: rethinking the primacy of experimental control in cognitive neuroscience. Neuroimage 222, 117254.
Nguyen, T., Zhou, T., Potter, T., et al., 2019. The cortical network of emotion regulation: insights from advanced EEG-fMRI integration analysis. IEEE Trans. Med. Imaging 38 (10), 2423–2433.
Niu, H., Zhu, Z., Wang, M., et al., 2019. Abnormal dynamic functional connectivity and brain states in Alzheimer's diseases: functional near-infrared spectroscopy study. Neurophotonics 6 (2), 025010.
Ochsner, K.N., Silvers, J.A., Buhle, J.T., 2012. Functional imaging studies of emotion regulation: a synthetic review and evolving model of the cognitive control of emotion. Ann. N. Y. Acad. Sci. 1251, E1–24.
Osaka, N., Minamoto, T., Yaoi, K., et al., 2015. How two brains make one synchronized mind in the inferior frontal cortex: fNIRS-based hyperscanning during cooperative singing. Front. Psychol. 6, 1811.
Pan, Y., Dikker, S., Goldstein, P., et al., 2020. Instructor-learner brain coupling discriminates between instructional approaches and predicts learning. Neuroimage 211, 116657.
Pan, Y., Novembre, G., Song, B., et al., 2018. Interpersonal synchronization of inferior frontal cortices tracks social interactive learning of a song. Neuroimage 183, 280–290.
Plichta, M.M., Herrmann, M.J., Baehne, C.G., et al., 2006. Event-related functional near-infrared spectroscopy (fNIRS): are the measurements reliable? Neuroimage 31 (1), 116–124.
Porro, C.A., Francescato, M.P., Cettolo, V., et al., 1996. Primary motor and sensory cortex activation during motor performance and motor imagery: a functional magnetic resonance imaging study. J. Neurosci. 16 (23), 7688–7698.
Scholkmann, F., Holper, L., Wolf, U., et al., 2013. A new methodical approach in neuroscience: assessing inter-personal brain coupling using functional near-infrared imaging (fNIRI) hyperscanning. Front. Hum. Neurosci. 7, 813.
Silvers, J.A., Wager, T.D., Weber, J., et al., 2015. The neural bases of uninstructed negative emotion modulation. Soc. Cogn. Affect. Neurosci. 10 (1), 10–18.
Tzourio-Mazoyer, N., Landeau, B., Papathanassiou, D., et al., 2002. Automated anatomical labeling of activations in SPM using a macroscopic anatomical parcellation of the MNI MRI single-subject brain. Neuroimage 15 (1), 273–289.
Wang, M.Y., Luan, P., Zhang, J., et al., 2018. Concurrent mapping of brain activation from multiple subjects during social interaction by hyperscanning: a mini-review. Quant Imaging Med. Surg. 8 (8), 819–837.

Xue, H., Lu, K., Hao, N., 2018. Cooperation makes two less-creative individuals turn into a highly-creative pair. Neuroimage 172, 527–537.
Yang, J., Zhang, H., Ni, J., et al., 2020. Within-group synchronization in the prefrontal cortex associates with intergroup conflict. Nat. Neurosci. 23 (6), 754–760.
Yucel, M.A., Luhmann, A.V., Scholkmann, F., et al., 2021. Best practices for fNIRS publications. Neurophotonics 8 (1), 012101.
Zhang, X., Noah, J.A., Dravida, S., et al., 2020. Optimization of wavelet coherence analysis as a measure of neural synchrony during hyperscanning using functional near-infrared spectroscopy. Neurophotonics 7 (1), 015010.
Zhang, Y., Ding, L., van Drongelen, W., et al., 2006. A cortical potential imaging study from simultaneous extra- and intracranial electrical recordings by means of the finite element method. Neuroimage 31 (4), 1513–1524.